Potential description of anomalous large angle scattering of α particles

A. S. B. Tariq, A. F. M. M. Rahman, S. K. Das, A. S. Mondal, M. A. Uddin, and A. K. Basak
Department of Physics, Rajshahi University, Rajshahi, Bangladesh

H. M. Sen Gupta
Department of Physics, University of Dhaka, Dhaka, Bangladesh

F. B. Malik
Department of Physics, Southern Illinois University, Carbondale, Illinois 62901
(Received 5 November 1998)

Angular distributions of the differential cross section of α elastic scattering by ^{24}Mg, ^{28}Si, and ^{30}Si nuclei have been studied for various incident energies. The observed enhancement of differential cross sections at back angles, usually known as anomalous large angle scattering (ALAS), cannot be explained in terms of the normal optical model potential. A molecular type or squared Woods-Saxon optical potential can account for the ALAS and produce satisfactory fits to the angular distributions. A mass dependence of the potential parameters in the range $A=24-30$ and energy variation in the region $E_\alpha=15-45$ MeV for the ^{28}Si target and 22–120 MeV for the ^{24}Mg target have been investigated. [S0556-2813(99)03104-0]

PACS number(s): 25.55.Ci, 24.10.Ht

I. INTRODUCTION

The nucleon-nucleus optical potential has been well understood for quite some time. However, the situation is not so clear in the case of the α-nucleus potential, particularly for light nuclei. α elastic scattering by these nuclei have some distinctive features that cannot be consistently explained by the ''usual'' Woods-Saxon (WS) type of optical potentials [1]. The inadequacy of the WS potential is obvious from the fits of α-silicon data by Jarzcyk *et al.* [2]. This has led Hodgson [3] to note that it has not yet been possible to obtain a really satisfactory global α-nucleus potential.

An important characteristic feature of experimental elastic scattering data by light nuclei at incident energies up to about 50 MeV is the unusual enhancement of cross section at large angles first noted for ^{16}O and ^{32}S targets by Correlli *et al.* [4]. It has since been observed for several other targets up to ^{48}Ca. This enhancement is commonly known as the anomaly in large angle scattering (ALAS). This phenomenon is most prominent in, but not unique to, $A=4n$ nuclei. At higher energies, the ALAS effect rapidly dies down giving rise to the so-called ''rainbow scattering'' characterized by a sharp decrease of cross section beyond a certain scattering angle.

The ALAS problem has, in the past, been approached from diverse directions using different local potentials. Some have tried to solve the problem by adding Hauser-Feshbach contributions to cross sections [2,5], which is, however, not expected to play a significant role at the energies above 20 MeV. Some added an l-dependent absorption [6,7], while others have used arbitrary WS^n ($n>2$) form factors [8]. None of these has been able to give a consistent and theoretically sound description of α-elastic scattering over a significant range of targets and energies.

The aim of this work is to examine the local potentials that can describe the α elastic scattering in the ALAS region in a consistent manner for a number of targets and over a considerable energy range. This analysis is restricted to the $1s$-$2d$ shell targets, for which complete angular distributions are available. For this analysis the squared WS potential used by Michel and his collaborators [9,10], henceforth referred to as the Michel potential, and the molecular potential [11,12] have been chosen. The rationale for the choice of the above two potentials is discussed in details in Sec. II but the key reason is that other types of potentials used failed to account for ALAS.

II. CHOICE OF POTENTIAL

The failure of the standard WS potential to account for the data for targets and energies considered herein is well documented, e.g., in [1,2]. A typical example is provided in Sec. III.

The squared Woods-Saxon Michel potential, i.e., WS^n with $n=2$, has provided the first successful description of α-^{40}Ca scattering from 20 to 170 MeV incident energy range [13]. With the inclusion of an energy dependent Gaussian factor to the real part, it has then been applied to α-^{16}O scattering data between 20 and 150 MeV incident energies [14] and produced excellent fits to the experimental data. Later investigations by the same group using this potential have also been successful in describing the α cluster structure in ^{44}Ti [15–17] and oscillations in the fusion excitation function [18]. Adding a slight angular momentum dependence to this potential and an increase in barrier height, it has also been possible to explain low energy data down to 3.5 MeV incident energy [19]. This purely phenomenological form of potential has been found to be very similar to the equivalent local potential obtained in microscopic analysis using the resonating group method [20]. The Michel potential including the Coulomb term $V_C(r)$ is comprised of the

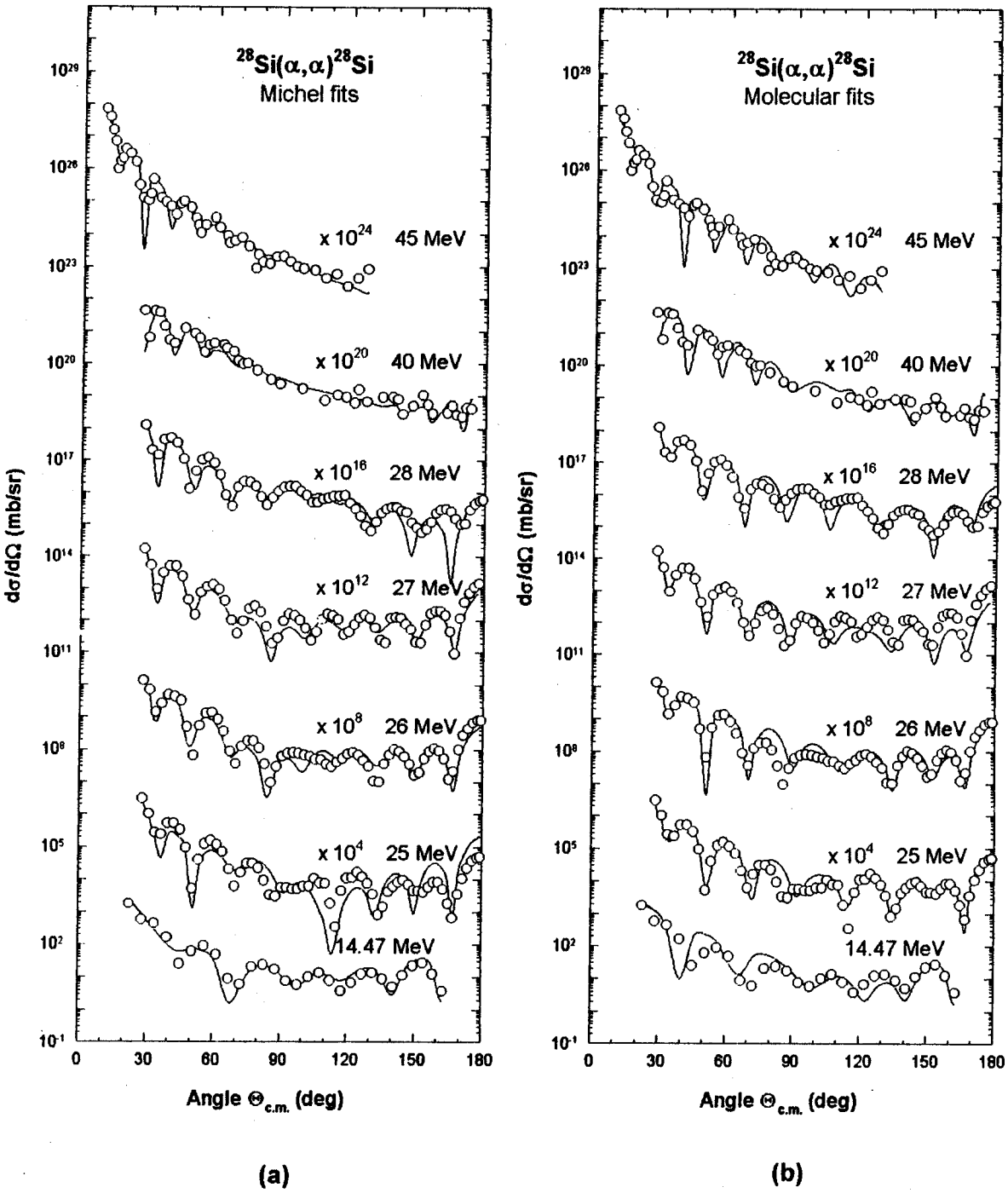

FIG. 1. (a) Michel-potential fits to the α-^{28}Si elastic scattering data at E_α(lab) = 14.47, 25, 26, 27, 28, 40, and 45 MeV and (b) molecular-potential fits to the same set of data. The molecular fits up to 28 MeV are basically reproductions from [12] for comparison with the fits using the Michel potential. The data are from [2,12,36].

following forms [14] of the real $V(r)$ and imaginary $W(r)$ parts:

$$V(r) = -V_0\left\{1+\alpha\exp\left[-\left(\frac{r}{\rho}\right)^2\right]\right\}\Big/\left[1+\exp\left(\frac{r-R_R}{2a_R}\right)\right]^2 + V_C(r), \tag{1}$$

with

$$V_C(r) = \left(\frac{Z_1Z_2e^2}{2R_C}\right)\left(3-\frac{r^2}{R_C^2}\right), \quad r \leqslant R_C,$$

$$= \frac{Z_1Z_2e^2}{r}, \quad r > R_C,$$

$$W(r) = -W_0\Big/\left[1+\exp\left(\frac{r-R_1}{2a_1}\right)\right]^2. \tag{2}$$

TABLE I. Michel potential parameters obtained from the analysis.

	E_α (MeV)	V_0 (MeV)	R_R (fm)	a_R (fm)	α	ρ (fm)	W_0 (MeV)	R_I (fm)	a_I (fm)	r_C(fm)	$J_R/4A$ (MeV fm^3)	$J_I/4A$ (MeV fm^3)
^{28}Si	14.47	21.0	5.0	0.60	18.0		13.9	3.85	0.65	1.3	886.35	22.41
	25.0				6.38		25.2				359.36	40.62
	26.0				8.39		33.1				450.52	53.35
	27.0				5.82	6.25	28.9				333.97	46.58
	28.0				5.23		32.5				307.21	52.39
	40.0				5.02		74.9				297.69	120.73
	45.0				4.34		93.5				266.85	150.71
^{30}Si	26.6	25.0	5.20	0.46	7.21	6.45	35.3	4.05	0.65	1.3	522.66	60.91
^{24}Mg	22.0	25.0	4.65	0.60	8.08		30.6	3.45	0.65	1.3	484.71	43.14
	28.0				7.60		39.6				460.58	55.83
	42.0				7.12		106.9				436.46	150.72
	50.0				7.00	5.85	128.3				430.43	180.89
	67.0				6.09		147.0				384.69	207.26
	81.0				5.43		158.4				351.52	223.33
	120.0				2.96		94.5				227.38	133.24

W_0 increases with energy due to the opening of more nonelastic channels, while the variation of α with energy reflects the energy dependence of the real part and thus, allows the analysis to be extended from energies exhibiting ALAS, into that relevant for rainbow scattering.

On the other hand, the molecular potential has its roots in the early works of Block and Malik [21] and others [22–24]. The initial motivation for proposing the molecular type of potential, has been the recognition of the role of the Pauli principle in heavy-ion-heavy-ion scattering. This kind of potential is characterized by a short range repulsive potential followed by an attractive region plus the usual Coulomb potential. Such potentials are expected from a many-body theory utilizing the energy-density functional method [23,25], even for the α-^{28}Si system [11,12,25]. Phase shift analyses, also, suggest such a potential for the ^{12}C-^{12}C and α-^{12}C systems [26,27]. Empirically, it has also provided good fits to the ^{12}C-^{12}C [28], ^{16}O-^{16}O [29] and other heavy-ion-heavy-ion elastic scattering data [30,31]. This type of potentials could cause substantial scattering at large angles, characteristic of ALAS, for the elastic scattering and nucleon transfer reaction [32]. This complex potential has the following forms [12] for real, $V(r)$, and imaginary, $W(r)$, parts:

$$V(r) = -V_0 \Big/ \left[1+\exp\left(\frac{r-R_0}{a}\right)\right] + V_1 \exp\left[-\left(\frac{r}{R_1}\right)^2\right] + V_C(r), \tag{3}$$

TABLE II. Molecular potential parameters obtained from the analysis.

	E_α (MeV)	V_0 (MeV)	R_0 (fm)	a (fm)	R_1 (fm)	V_1 (MeV)	W_0 (MeV)	R_W (fm)	R_C (fm)	$J_R/4A$ (MeV fm^3)	$J_I/4A$ (MeV fm^3)
^{28}Si	14.47	26.0	5.35	0.34	2.80	42.0	1.0	4.00	9.35	109.01	3.16
	25.0						14.0				44.31
	26.0						14.5				45.89
	27.0						15.0				47.47
	28.0						18.0				56.96
	40.0						24.0				75.95
	45.0						29.5				93.36
^{30}Si	26.6	26.3	5.45	0.34	2.90	42.5	17.5	4.10	9.45	112.79	55.63
^{24}Mg	22.0	25.4	5.15	0.34	2.60	41.0	13.0	3.80	9.15	116.10	41.20
	28.0						18.0				57.05
	42.0						26.0				82.40
	50.0						27.0				85.57
	67.0						29.0				91.91
	81.0						33.0				104.58
	120.0						35.0				110.92

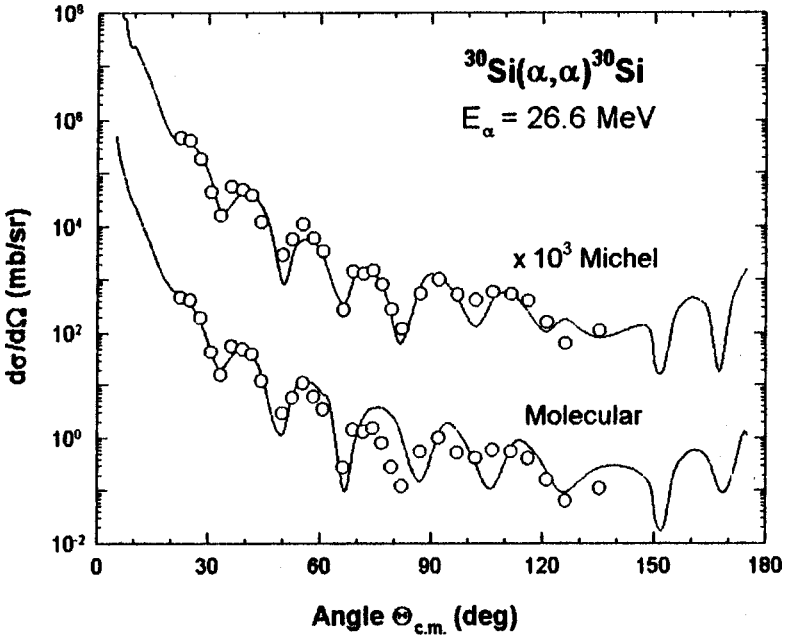

FIG. 2. Michel- and molecular-potential fits to the α-^{30}Si elastic scattering data at 26.6 MeV of [37].

$$W(r) = -W_0 \exp\left[-\left(\frac{r}{R_W}\right)^2\right]. \quad (4)$$

Here, W_0 is the only energy dependent parameter within moderate energy intervals. However, the real part might need to be varied at different energy intervals if the analysis is extended to a large energy domain.

As noted already this potential has been successfully used in the description of the α-^{28}Si elastic scattering in the ALAS region for incident energy interval of 21 to 28 MeV with an energy independent real potential [12]. Through a simple scaling procedure, as described in Sec. III, it could also describe reasonably well the elastic scattering of α particles from ^{32}S and ^{34}S isotopes. Therefore the applicability of such a potential to other targets and its target and energy dependence have also been a part of this investigation.

In a preliminary search, Manngård *et al.* [12] failed to describe the elastic α-^{28}Si scattering data using the Michel potential. It is therefore intriguing to examine whether such an overwhelmingly successful potential is truly a failure in the case of a ^{28}Si target, and if not so, what would be the nature of its energy and target dependence.

III. ANALYSIS AND DISCUSSION

It has been noted that angular distributions with only small or large angle data are not sufficient for a definite determination of the optical potential [33]. Therefore, data containing cross sections over a complete range of angles are chosen for this analysis. For the fitting of the angular distributions, the chi-square minimization code MINUIT [34] has been used in conjunction with the optical model code SCAT2 [35] to find the parameters of the potentials. The code SCAT2 had to be modified to incorporate the Michel and molecular potentials. The least squared method is used as a guide and tool in locating the best-fit parameters, but the final choice

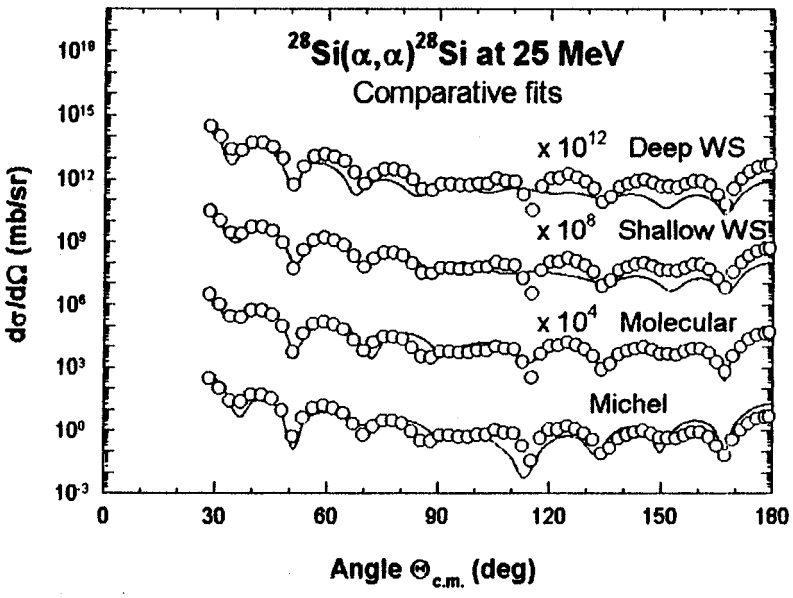

FIG. 3. Fits to the α-^{28}Si elastic scattering data of [2] at 25 MeV with shallow WS, deep WS, molecular, and Michel potentials. The inadequacy of the WS potentials is evident at large angles.

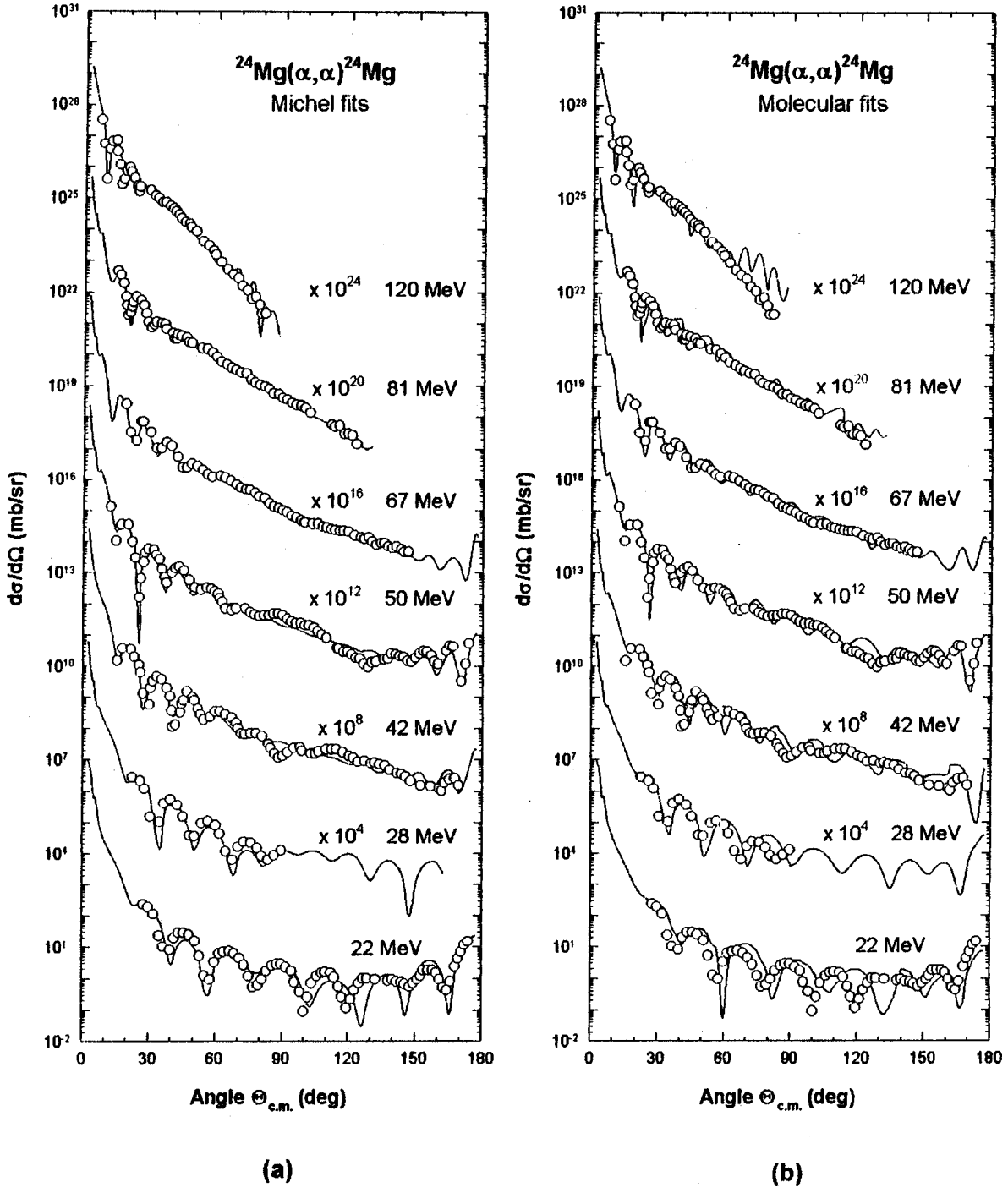

FIG. 4. (a) Michel-potential fits to the α-^{24}Mg elastic scattering data at $E_\alpha(\text{lab}) = 22$, 28, 42, 50, 67, 81, and 120 MeV and (b) molecular-potential fits to same set of data. Data are from [39].

has been made visually, since it is quite possible for a physically defective distribution, to have a set of parameters with a lower χ^2 value than a more physically meaningful one.

Unlike the results of the preliminary search of [12], it is possible to obtain a reasonable fit to the 14.47 MeV α-^{28}Si data of [12], the 25–28 MeV data of [2] and the 40 and 45 MeV data of [36] using the Michel potential with α and W_0 as the only varying parameters. It is also possible to extend the analysis of [12] to the 40 and 45 MeV data without any variation of the real part of the molecular potential. The fits with the Michel and molecular potential are shown in Fig. 1, while the values of the potential parameters are given in Tables I and II.

It is also possible to fit the 26.6 MeV data for ^{30}Si of Siemaszko *et al.* [37] using both the potentials as shown in Fig. 2. In case of the molecular potential the suggested scaling [11] of the parameters, noted below, has been used:

$$R_i = R_\alpha + r_0 A_\tau^{1/3} \quad (i = 0, 1, W, \text{ and } C), \tag{5}$$

with $r_0 = 1.35$ fm, and

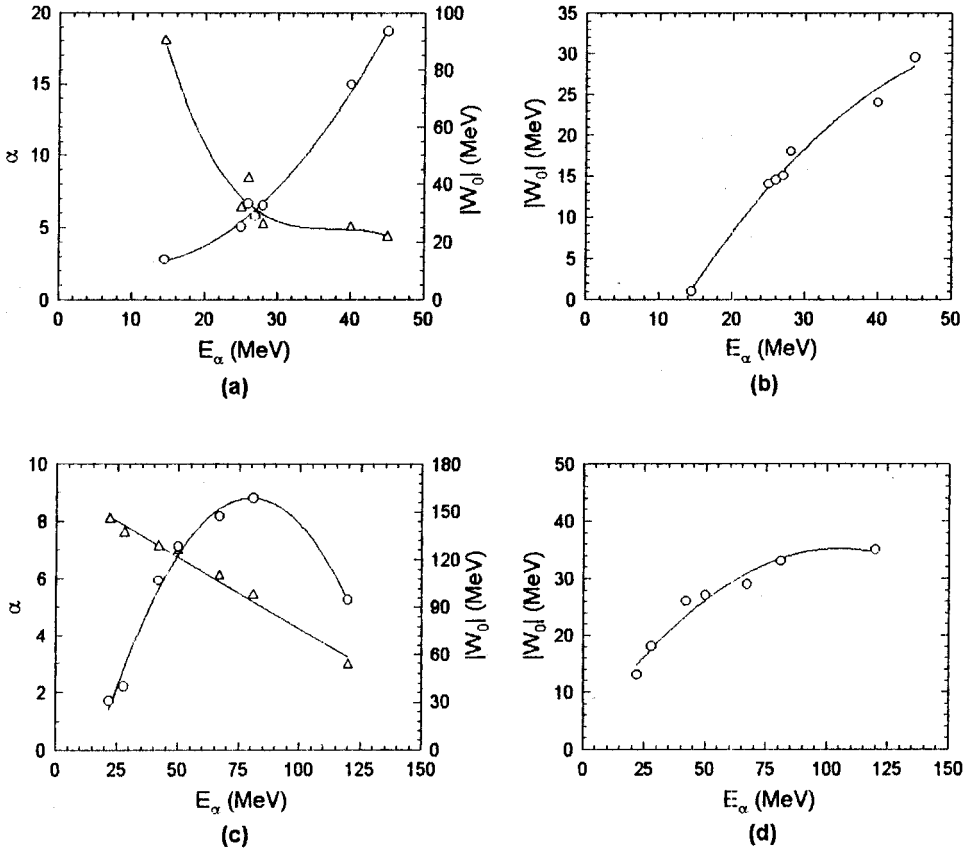

FIG. 5. Energy dependence of (a) Michel parameters for ^{28}Si, (b) molecular parameters for ^{28}Si, (c) Michel parameters for ^{24}Mg and (d) molecular parameters for ^{24}Mg. Triangles are for α and circles for W_0.

$$V_i = b_i[4^{2/3} + A_\tau^{2/3} - (4 + A_\tau)^{2/3}] \quad (i = 0,1). \tag{6}$$

Thus, the scaling could be applied successfully for nuclei adjacent to ^{28}Si.

In Fig. 3, fits to the α-^{28}Si data at 25 MeV are provided using the standard optical model (WS), the Michel and the molecular potentials for the sake of comparison. Clearly, the standard optical potential is not suitable. The situation is similar at other energies.

From the fits to the angular distributions, one can note that there is little to choose between the deep Michel and shallow molecular potentials. Since, the Goldberg criterion [38] requires analysis of data in the rainbow scattering region for the elimination of the discrete ambiguity, which are not available for the α-^{28}Si system, the analysis is extended to the 22–120 MeV α-^{24}Mg data of Neu *et al.* [39]. Here again it is possible to obtain almost equally good fits with both the potentials. The fits are shown in Fig. 4, while the potential parameters alongwith the volume integrals are given in Tables I and II.

Looking at the energy dependence of the parameters (Fig. 5) one observes that they follow a regular pattern. There is, however, some scope for improvement. For example, the values of α in the Michel fits to ^{28}Si at 25, 27, and 28 MeV are a bit too small, while that for 14.47 MeV is perhaps too large compared to the one expected from the α-^{24}Mg case. Its dependence on energy has also departed from the expected linear behavior [14]. One also notes that the corresponding values of the real volume integral depart from the line drawn through the points for ^{24}Mg (Fig. 6). The α-^{24}Mg Michel potential derived here is probably more reliable due to its extension into higher energy regions. For the α-^{24}Mg scattering the parameter α can be represented by the linear relation

$$\alpha = 9.28 - 0.05E_\alpha, \tag{7}$$

while the corresponding real volume integral has the linear energy dependence

$$J_R/4A = 544.8 - 2.53E_\alpha, \tag{8}$$

which has a slightly higher slope and intercept than those derived for the ^{40}Ca [13] and the ^{16}O cases [14]. The drop of the Michel W_0 at higher energies is also puzzling.

With the exception of the 120 MeV ^{24}Mg data beyond 60° the molecular potential too, describes all the data quite well. This potential is found to have a smooth variation with energy. Within the energy interval considered here, W_0 is found to be approximately given by

$$W_0 = -20.85 + 1.73E_\alpha - 0.01E_\alpha{}^2$$

$$\text{for } ^{28}\text{Si between 14 and 45 MeV}, \tag{9}$$

$$W_0 = -2.46 + 0.62E_\alpha - 0.003E_\alpha{}^2$$

$$\text{for } ^{24}\text{Mg between 22 and 120 MeV}. \tag{10}$$

It is a surprise to be able to fit all the data with the same real potential. The volume integral for the real part, thus, has no energy dependence and is about 110 MeV fm^3 per nucleon pair for all the targets. The volume integrals for the imagi-

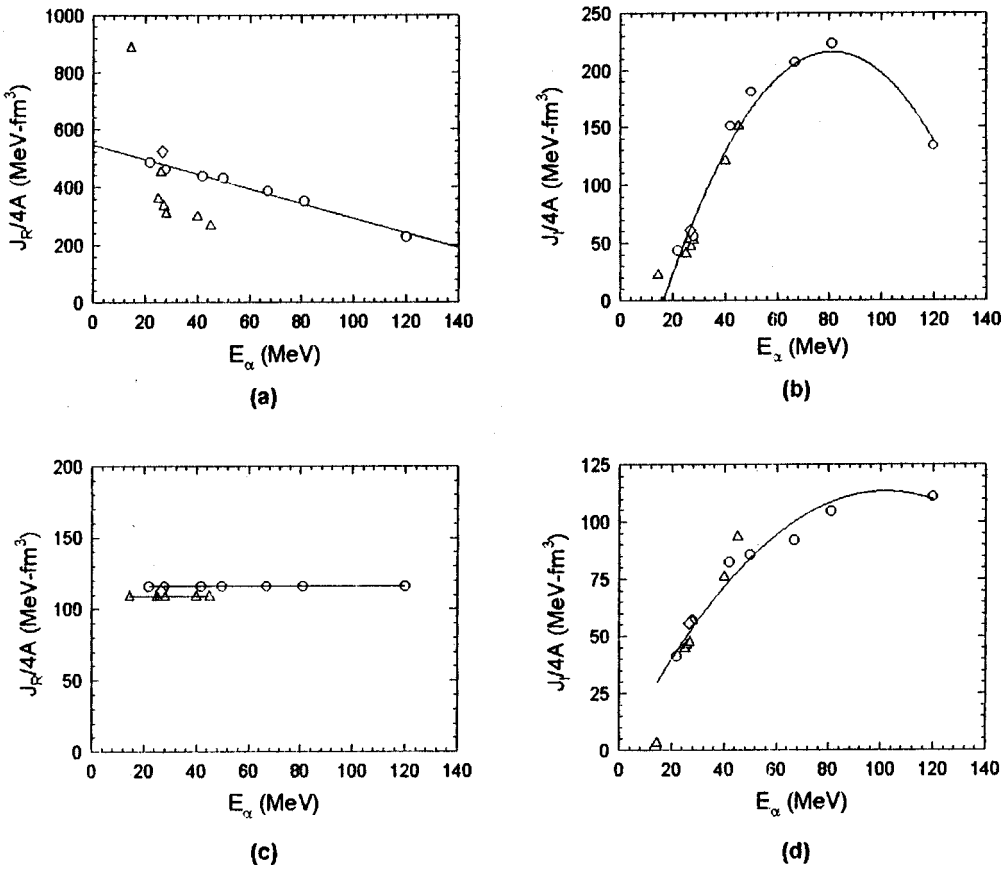

FIG. 6. Volume integrals per nucleon pair as a function of energy for the (a) Michel real, (b) Michel imaginary, (c) molecular real, and (d) molecular imaginary potentials. Circles are for ^{24}Mg, triangles for ^{28}Si, and diamonds for ^{30}Si.

nary part for all the targets taken together can be parametrized by the following quadratic relation:

$$J_I/4A = 2.23E_\alpha - 0.01E_\alpha{}^2. \tag{11}$$

It is observed that the real part of the potential is almost completely determined by the position of the forward peaks, while the backward angles determine the strength of the imaginary part. Due to the VR^n type of continuous ambiguity, one should preferably keep the geometry fixed while searching for the depths. The diffuseness is found to have no meaningful energy or target dependence for both the potentials. A variation of the diffuseness is found to affect only the magnitudes of the oscillations in angular distributions. It is

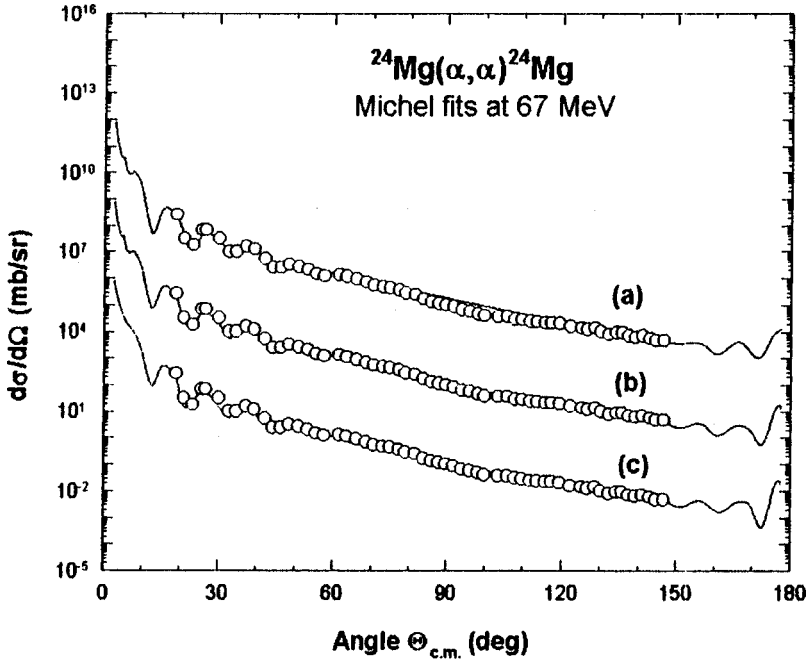

FIG. 7. Three pairs of α-W_0 values giving similar fits: (a) $\alpha = 5.00$, $W_0 = 115.0$ MeV, (b) $\alpha = 6.09$, $W_0 = 147.0$ MeV, and (c) $\alpha = 7.00$, $W_0 = 162.0$ MeV.

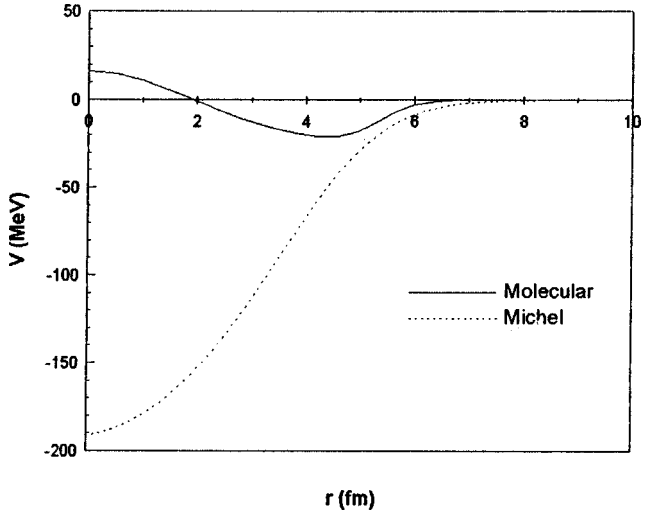

FIG. 8. Comparison of the real part of the Michel and molecular potentials for ^{28}Si at 26 MeV.

possible to fit all the data without any energy or target dependence in the diffuseness, with the sole exception of the Michel fit to the ^{30}Si data where a_R had to be adjusted from 0.46 to 0.60 fm.

There are, still, ambiguities in the choice of the real and imaginary parts of the Michel potential. For example, the 67 MeV α scattering data by ^{24}Mg can be fitted with more than one pair of α-W_0 values, as shown in Fig. 7. This ambiguity may be used to smoothen the energy evolution of the volume integrals and lead to further studies in the field of dispersion relations. No such clear ambiguity is found for the molecular potential.

As mentioned earlier, the Michel potential is a deep one ($J_R/4A \sim 400$ MeV fm^3 per nucleon pair), while the molecular potential is quite shallow ($J_R/4A \sim 110$ MeV fm^3 per nucleon pair). The plots of the two potentials describing the scattering from ^{28}Si at 26 MeV (Fig. 8) show that they differ considerably in the interior region ($r < 5$ fm) but have similar magnitudes at the surface. The implication may be that the surface region is primarily determining the scattering. At the same time, it also means that the potential is not well determined, or transparent, in interior regions. This has led us to perform the notch test [14] where the real part of the potential is perturbed by introducing small Gaussian notches through multiplication by the factor

$$f(r;S,b,d) = 1 - d \exp\{-[(r-S)/b]^2\}. \qquad (12)$$

The notch is given a depth of 10% ($d = 0.1$) and width of about 1 fm ($b = 0.5$ fm), while S has been varied from 0 to 10 fm in 0.5 fm steps. The effect is judged by the radial dependence of the normalized variation of chi-square, $[(\chi^2 - \chi_0^2)/\chi_0^2]^2$. The results obtained (Fig. 9) show that the scattering really does occur mostly from the surface region at 4–6 fm, giving an explanation for the discrete ambiguity. In this region the two potentials are similar, but not identical. The fact that they still produce similar scattering cross-sections might be reconciled if one considers their different absorptive strengths. The transparency of the potential is, as expected, found to be less than that for ^{16}O and ^{40}Ca (down to $\sim$4 fm as opposed to $\sim$2 fm in those cases) [13,14].

IV. CONCLUSION

Both the Michel and molecular potentials have been shown to give a satisfactory description of the alpha elastic scattering for targets in the mid-sd shell region including ALAS, without any resonance contribution. The same potentials could also describe the rainbow scattering for ^{24}Mg at higher energies with reasonable variations of the parameters. The inclusion of resonances explicitly may be needed at lower incident energies [31].

Taking earlier works together [13–19], the Michel potential already seems to be valid over quite a large region spanning targets with $A = 16$ to 44 and α energies as low as 3.5 MeV up to 166 MeV. The molecular potential has also proven to be valid over quite a wide energy interval. Both the potentials now have a predicting power over a large energy range which is very helpful in analyzing inelastic and particle transfer data. With a more rigorous and comprehensive analysis along the lines mentioned in the preceding discussion, it seems possible, that both these potentials could prove to be good global potentials.

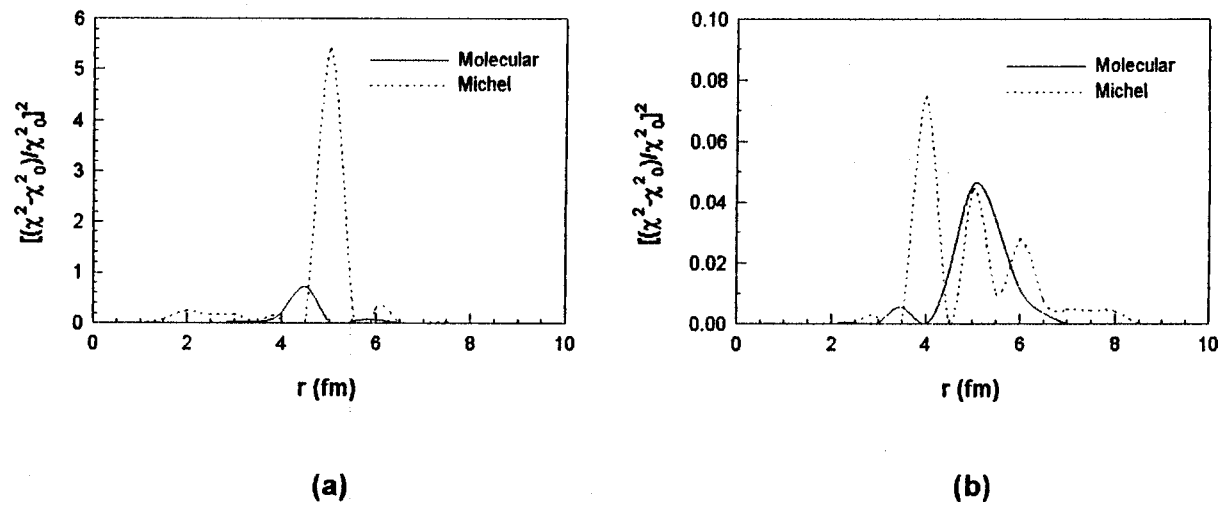

FIG. 9. Notch test results for α-^{28}Si at (a) 26 MeV and (b) 45 MeV.

However, according to Satchler [40] the real test of a potential is in the description of non-elastic processes. Preliminary results from our group already indicate that the molecular potential seems to have an edge over the Michel potential when it comes to the description of inelastic scattering and transfer reactions. This is in accordance with Baye's observation [41] which suggests that a shallow potential with a singularity, which the molecular potential bears, eliminates the unphysical states of the bound system and hence, is expected to produce a better description of non-elastic processes.

We began this paper with Hodgson's comment on the absence of a satisfactory global α-nucleus potential. As we finish, one can see the promise of this vacuum being filled. The applicability of these potentials to not only elastic scattering, but inelastic scattering and reactions as well, is therefore worth further investigation.

ACKNOWLEDGMENTS

The interests and assistance of Professor P. E. Hodgson and Professor M. Brenner are gratefully acknowledged. This research was made possible by Grant No. INT-9808892 of the U.S. National Science Foundation. This grant is thankfully acknowledged.

[1] M. Brenner, in *Clustering Phenomena in Atoms and Nuclei*, edited by M. Brenner, T. Lönnroth, and F. B. Malik (Springer-Verlag, Berlin, Heidelberg, 1992), p. 327.
[2] L. Jarczyk, B. Maciuk, M. Siemaszko, and W. Zipper, Acta Phys. Pol. B **7**, 531 (1976).
[3] P. E. Hodgson, Oxford Report, OUNP-94-09 (1994).
[4] J. C. Correlli, E. Bleuler, and J. Tandem, Phys. Rev. **116**, 1184 (1959).
[5] W. Wuhr, A. Hoffman, and G. Phillipp, Z. Phys. **269**, 365 (1974).
[6] A. W. Obst and K. W. Kemper, Phys. Rev. C **5**, 1705 (1972).
[7] J. Lega and P. C. Macq, Nucl. Phys. **A218**, 429 (1974).
[8] B. Xiumin, L. Shiming, W. Yuanda, Y. Rongfang, H. Bingyin, and S. Zuxun, Chin. Phys. **6**, 645 (1986).
[9] F. Michel, Phys. Rev. C **13**, 1446 (1976).
[10] F. Michel and R. Vanderpoorten, Phys. Lett. **82B**, 183 (1978).
[11] P. Manngård, M. Brenner, I. Reichstein, and F. B. Malik, in *Proceedings of the 5th International Conference on Nuclear Reaction Mechanisms*, Varenna, Italy, edited by E. Gadioli (Ricerca Scientifica ed Educazione Permanente, University of Milan Press, Milan, 1988), Suppl. 66, p. 385.
[12] P. Manngård, M. Brenner, M. M. Alam, I. Reichstein, and F. B. Malik, Nucl. Phys. **A504**, 130 (1989).
[13] Th. Delbar, Gh. Grégoire, G. Paic, R. Ceuleneer, F. Michel, R. Vanderpoorten, A. Budzanowski, H. Dabrowski, L. Friendl, K. Grotowski, S. Micek, R. Planeta, A. Strzalkowski, and A. Eberhard, Phys. Rev. C **18**, 1237 (1978).
[14] F. Michel, J. Albinski, P. Belery, Th. Delbar, Gh. Gregoire, B. Tasiaux, and G. Reidemeister, Phys. Rev. C **28**, 1904 (1983).
[15] F. Michel, G. Reidemeister, and S. Ohkubo, Phys. Rev. Lett. **57**, 1215 (1986).
[16] S. Ohkubo, Phys. Rev. C **36**, 551 (1987).
[17] F. Michel, G. Reidemeister, and S. Ohkubo, Phys. Rev. C **37**, 292 (1988).
[18] F. Michel, G. Reidemeister, and S. Ohkubo, Phys. Rev. C **34**, 1248 (1986).
[19] F. Michel, G. Reidemeister, and Y. Kondo, Phys. Rev. C **51**, 3290 (1995).
[20] T. Wada and H. Horiuchi, Phys. Rev. Lett. **58**, 2190 (1987).
[21] B. Block and F. B. Malik, Phys. Rev. Lett. **19**, 239 (1967).
[22] R. J. Munn, B. Block, and F. B. Malik, Phys. Rev. Lett. **21**, 159 (1968).
[23] K. Brueckner, J. R. Buchler, and M. M. Kelly, Phys. Rev. **173**, 944 (1968).
[24] W. Scheid, R. Ligensa, and W. Greiner, Phys. Rev. Lett. **21**, 1479 (1968).
[25] F. B. Malik and I. Reichstein, in *Clustering Phenomena in Atoms and Nuclei*, edited by M. Brenner, T. Lönnroth, and F. B. Malik (Springer-Verlag, Berlin, Heidelberg, 1992), p. 126; Phys. Lett. **37B**, 344 (1971).
[26] M. M. Alam and F. B. Malik, Nucl. Phys. **A524**, 88 (1991).
[27] M. M. Alam and F. B. Malik, Phys. Lett. B **237**, 14 (1990).
[28] Q. Haider and F. B. Malik, J. Phys. G **7**, 1661 (1981).
[29] L. Rickertsen, B. Block, J. W. Clark, and F. B. Malik, Phys. Rev. Lett. **22**, 951 (1969).
[30] Z. F. Shehadah, Doctoral dissertation, Southern Illinois University at Carbondale, 1994.
[31] M. Brenner, K.-M. Källman, Z. Maté, T. Vertse, and L. Zolnai, Heavy Ion Phys. **2**, 269 (1995).
[32] F. Schmittroth, W. Tobocman, and A. A. Golestaneh, Phys. Rev. C **1**, 377 (1970).
[33] A. Budzanowski, L. Jarczyk, L. Kamys, and A. Kapuscik, Nucl. Phys. **A265**, 461 (1976).
[34] F. James and M. Roos, Comput. Phys. Commun. **10**, 343 (1975).
[35] O. Bersillon, SCAT2 code, NEA 0289, 1988.
[36] S. Roy, T. Dey, A. Goswami, S. N. Chintalapadi, and S. R. Banerjee, Phys. Rev. C **45**, 2904 (1992).
[37] M. Siemaszko, J. Czakanski, A. Grzeszczuk, K. Jankowski, J. Kisiel, B. Kozlowska, A. Surowiec, W. Zipper, and A. Budzanowski, J. Phys. G **20**, 1789 (1994).
[38] D. A. Goldberg and S. M. Smith, Phys. Rev. Lett. **29**, 500 (1972).
[39] R. Neu, S. Welte, H. Clement, H. J. Hauser, G. Staudt, and H. Müther, Phys. Rev. C **39**, 2145 (1989).
[40] G. R. Satchler, *Proceedings of the International Conference on Reactions between Complex Nuclei*, Nashville (North-Holland, Amsterdam, 1974), p. 171.
[41] D. Baye, Phys. Rev. Lett. **58**, 2738 (1987).